OPTOELECTRONICS AND ADVANCED MATERIALS – RAPID COMMUNICATIONS Vol. 14, No. 11-12, November-December 2020, p. 538-541

Accurate evaluation of electron energy density and electron concentration in quantum wells

S. SAYGI*, K. O. SAYGI
Department of Physics, Faculty of Art and Science, Gaziosmanpasa University, Tokat, Turkey

In this article, we propose an approach to calculate the effective electron concentration and electron energy density in multilayer high electron mobility transistors (HEMT). After utilizing an interesting mathematical change to achieve realistic results, numerical modeling was applied to model devices with algebraic computer language. The simulation results for band structure and electron density profile are comparable with those of other numerical calculations.

(Received May 30, 2020; accepted November 25, 2020)

Keywords: Electron concentration, Modeling of devices, HEMT, Incomplete Gamma functions, Numerical modeling

1. Introduction

Quantum well devices have been used as microwave oscillators, switches, attenuators, and amplifiers for discrete ultra-high-speed circuit elements. The devices can also be incorporated into a monolithic integrated circuit in modern technology [1]. The high power and high frequency requirements are due to transistor devices based on semiconductor materials with both high breakdown voltage and high electron velocity. Two advantages of these devices can be counted. The first is the presence of a wide bandgap, which leads to high breakdown voltage and high saturation velocity. The second is the existence of heterostructures with high conduction band offset and high piezoelectricity, which results in high sheet carrier densities [2]. The ability of nitrate-based alloy semiconductor materials to form a heterojunction is unlimited compared to other semiconductor materials made from alloys.

The physical phenomena that occur in such a micro-device require precise physical models to characterize the functioning of the device and crucially optimize the structure. Modeling the progression requires many steps that correspond to the functionality of the device. The equations for the physical modeling, essentially differential equations, are defined by related approaches. In [3], a detailed description and the modeling equations are provided. Cole [4] suggested acceptable physical equations based on aspects of quantum and statistical mechanics. Cole also showed additional complexity and how to solve the Schrödinger and Poisson equations. The solution to the equations is based on the calculation of the electron density and electron energy densities of the components using certain integrals with approximate realistic results for device modeling.

Papers [5] and [6] proved a new analytic approach to formulas included in the analytical forms of Cole's device modeling, using incomplete gamma functions. In Mamedov's article, the solutions did not apply to the devices; it showed how the results could be converged towards the model. For the purpose of the present paper, a highly precise analytic method will be applied to a multilayer device to optimize the design. The device's band structure and electron density will be depicted.

2. Definitions and formulations

As a new aspect of our work, an algebraic computer language is implemented for the electron densities and the electron energy density. Later, they are reduced to incomplete gamma functions, $I_r(a,b)$, and then converted into the Fermi integrals. Multilayered High Electron Mobility Transistors, HEMT, are appropriate for the application of the formulated criterion.

For the structure, the electrons confined in a channel are calculated by solving the Poisson equation as follows.

$$\frac{d^2}{dx^2}\varepsilon_0\varepsilon_r(x)\phi(x) = -q\left[N_D - n\right] \tag{1}$$

The right side of the equation needs the electron density n. The total electron density for a layer structure results from the contribution of the subbands and from the bulk electron density [4].

$$n = n_s + n_b \tag{2}$$

n_s and n_b are defined from outside the potential well as

$$n_s = 0\,, \qquad n_b = N_{cb}F_{1/2}\left(\frac{q\,(E_F - E_C}{k_BT}\right), \tag{3}$$

and from inside the potential well as

$$n_s = N_{c2}\sum_{i=0}^{L-1}\left|\xi\right|^2 \ ln\left(1+e^b\right),$$

$$n_b = N_{cb} I_{1/2}\left(\frac{q\left(E_F - E_{top}\right)}{k_B T}, \frac{q\left(E_{top} - E_C\right)}{k_B T}\right). \tag{4}$$

For the non-degenerated case, the expressions corresponding to energy density are given as

$$w_s = 0 \ \text{ and } \ w_b = \frac{3}{2} N_{cb}\left(k_B T\right) F_{1/2}\left(\frac{q\left(E_F - E_c\right)}{k_B T}\right) \tag{5}$$

outside the quantum well, while in the quantum well, they are given as

$$w_s = N_{cb}\left(k_B T\right)\sum_{\lambda \le E_{top}}\left|\xi_{j(y)}\right|^2 I_1\left(\frac{q\left(E_F - \lambda_j\right)}{k_B T}, \frac{q\left(\lambda_j - E_C\right)}{k_B T}\right) \tag{6}$$

$$w_b = \frac{3}{2} N_{cb}\left(k_B T\right) I_{3/2}\left(\frac{q\left(E_F - E_{top}\right)}{k_B T}, \frac{q\left(E_{top} - E_C\right)}{k_B T}\right) \tag{7}$$

where the electron concentration for related material is

$$N_{cb} = 2\left(\frac{m^* k_B T}{2\,\pi\,\hbar^2}\right). \tag{8}$$

In equations (5) through (7), $w_s + w_b$ is the total energy and is a constant number in the case of electrons. The potential well is formed near the interface. Therefore, the Schrödinger equation needs the solution of the Poisson equation solution.

$$-\frac{\hbar^2}{2}\frac{d}{dx}\left(\frac{1}{m^*}\frac{d}{dx}\xi_i\right) + \left(V_{xc} + E_h - q\psi\right)\xi_i = q\lambda_i\xi_i \tag{9}$$

V_{xc} is exchange correlation energy, $m^* = \left(0.067 + 0.083\,x\right)m_e$ is the effective electron mass, and x is the material concentration. The band offset of the different layers is $E_h = 0.65\left(1.155\,x - 0.37\,x^2\right)$ and the permittivity of the material is $\varepsilon_r = 13.18 - 3.12\,x$.

From now on, the task consists of obtaining the formulas' incomplete gamma functions, $J_r\left(a,b\right)$ and $F_r\left(a\right)$, which appear in equations (2) to (7), using the binomial expansion theorem.

$$f_m\left(n\right) = \begin{cases} \dfrac{n\left(n-1\right)\ldots\left(n-m+1\right)}{m!} & \text{for integer n} \\ \dfrac{\left(-1\right)^m \Gamma\left(m-n\right)}{m!\,\Gamma\left(-n\right)} & \text{for noninteger n} \end{cases} \tag{10}$$

In the extraction of the formulas, the recurrence relations for gamma functions were used. By writing a Mathematica code to demonstrate the numerical results [7], we have $J_r\left(a,b\right)$ and $F_r\left(a\right)$ as follows:

$$J_r(a\,,b) = \frac{1}{\Gamma\left(r+1\right)}\left[\frac{b^{r+1}}{r+1} + \lim_{N\to\infty}\sum_{i=1}^{N} fi\left(-1\right)K_i\left(r,b\right)\right] \tag{11}$$

$$F_r\left(a\right) = \frac{1}{\Gamma\left(r+1\right)}\left[\frac{a^{r+1}}{r+1} + \lim_{N\to\infty}\sum_{i=1}^{N} fi\left(-1\right)K_i\left(r,a\right)\right] + \lim_{N'\to\infty}\sum_{j=1}^{N'} f_j\left(-1\right)e^{a(1+j)}\frac{\Gamma\left(r+1,\ a\left(j+1\right)\right)}{\left(j+1\right)^{r+1}} \tag{12}$$

The expression $K_i\left(r,a\right)$ in equations (11) and (12) is determined by the relation

$$K_i\left(r,a\right) = e^{-ai}\sum_{j\to 1}^{L}\frac{a^{r+j+1}}{\left(r+j+1\right)j!}i^j \tag{13}$$

$\Gamma\left(\alpha,x\right)$ are incomplete gamma functions.

3. Calculations and discussion

Fig. 1 schematically shows a typical conduction band profile for an HEMT device for comparison with the predicting model. The device was formed with a doped ternary compound AlGaAs layer, 20 nm thin, and then an undoped ternary AlGaAs spacer layer, a few nm deep, was placed over it. Finally, a binary buffer GaAs layer, 200 nm deep, was positioned further down. The composition of Alin doped layer was 0.3. The other physical parameters related to the device can be found in other texts.

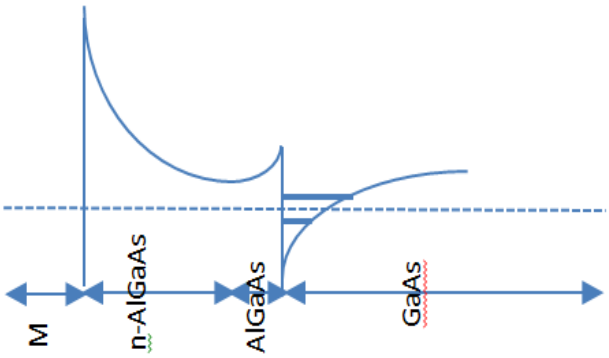

Fig. 1. Schematic Diagram of the Conduction Band of a HEMT

The profile of the conduction band of such a quantum well device modified by the incomplete gamma functions $I_r(a,b)$ and then converted into the Fermi integrals method is presented graphically in Fig. 2. The modified model result indicates a quantum well at the heterostructure. Electrons in the buffer layer showed triangular type confinement as expected. As indicated by the conduction band profile, a spacer layer was necessary to prevent Coulombic interactions between electrons and ionize dopant atoms. In the absence of this layer, the electron distribution might possibly spill out into the metal. The electron density as a key characteristic of quantum well devices was at the maximum value in the region near the metal semiconductor interface. We note that the conduction band disruption occurred where the range of maximum electron density was 23 nm.

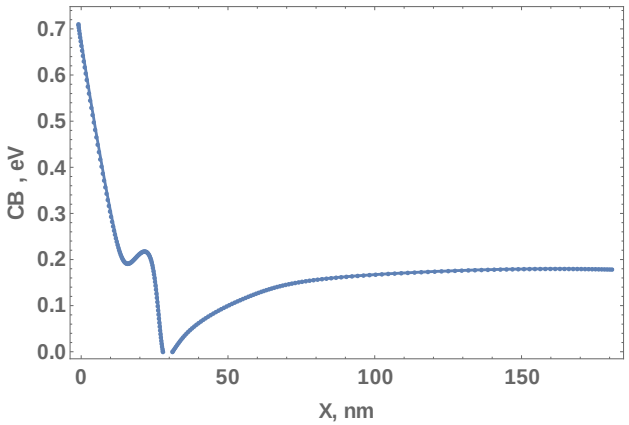

Fig. 2. Conduction Band Profile of the modified model

In Fig. 3, the constructed model graphically shows the expected electron density. We assumed that the contributions to the electron density originated from the subbands caused by the AlGaAs layer and the bulk electron density caused by the GaAs layer. The current voltage characteristics, which were not dealt with in this work, could also be verified precisely on the basis of our mathematical substitutions of the proposed formulas and the knowledge of the electron distribution. When we compared our results with other calculations as shown in [3], the consistency of the method was confirmed. The results have been adapted properly to experimental data as shown in [8].

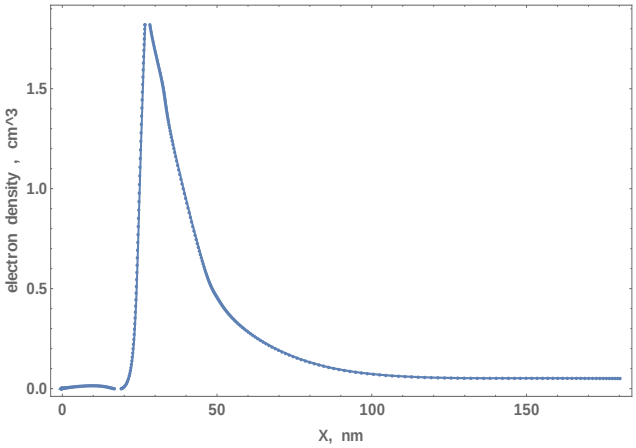

Fig. 3. Electron Density of the modified model

The numerical results of our modified model provided an advantage in two-dimensional device simulation in which the number of equations and unknowns are considerable to be solved. The modified formulas have been written in algebraic computer language, and Mathematica codes of the formulas $J_r(a,b)$ and $F_r(a)$ are provided in the appendix.

3. Conclusions

We introduced a new analytic approach to the work of [4] that gives realistic results for modeling the devices. The execution of the formulas after reduction to incomplete gamma functions and then conversion to the Fermi integrals method provided significant advantages in terms of numerical efficiency and reasonable accuracy compared with complex methods. The simple exact expressions obtained for the model reduce the computational burden. The results can also help to determine device current-voltage characteristics. In addition, one can numerically estimate AC small-signal parameters from large signal data at great computational speed. The expressions obtained for the simulation of semiconductor device are exact and quickly predictable.

Appendix

Incomplete gamma functions, $J_r(a,b)$ and $F_r(a)$, may be written in Mathematica code as follows.

$$K_{ira}[i,r,a] = E^{-ai}\sum_{j=0}^{s}\frac{a^{r+j+1}}{(r+j+1)\,j!}i^{j}; \quad (14)$$

$$F_{ra}[r,a] = \frac{1}{Gamma[r+1]}\left(\frac{a^{r+1}}{r+1}\right) + \sum_{i=1}^{s} Binomial[-1,i]K_{ira}[i,r,a] + \sum_{j=0}^{s} Binomial[-1,i]E^{a(j+1)}\frac{Gamma[r+1,a(j+1)]}{(j+1)^{r-1}}; \quad (15)$$

$$I_{rab}[r,a,b] = \frac{1}{Gamma[r+1]}\left(\frac{b^{r+1}}{r+1}\right) + \sum_{i=1}^{s} Binomial[-1,i]E^{ai}K_{ira}[i,r,a]; \quad (16)$$

References

[1] M. N. Horenstein, "Microelectronic Circuits and Devices", Pearson, 1996.

[2] B. Streetman, S. Banerjee, "Solid State Electronic Devices", 6th ed., Prentice Hall, 2005.

[3] C. M. Snowden, R. E. Miles, "Compound Semiconductor Device Modelling", 1st ed. Springer, 1993.

[4] E. A. B. Cole, J. Phys. Condens. Matter. **13**, 515 (2001).

[5] B. A. Mamedov, Comput. Phys. Commun. **178**(9), 673 (2008).

[6] I. I. Guseinov, B. A. Mamedov, J. Math. Chem. **36(**4), 341 (2004).

[7] S. Saygi, B. A. Mamedov, J. Comput. Electron. **13**(2), 370 (2014).

[8] K. A. Christianson, W. T. Anderson, Science **39**(12), 1757 (1996).

*Corresponding author: salih.saygi@gop.edu.tr